



Cite this: *Mater. Adv.*, 2022, **3**, 8792

Received 22nd August 2022,
Accepted 14th October 2022

DOI: 10.1039/d2ma00873d

rsc.li/materials-advances

Promotion of Suzuki–Miura reaction under bimetallic green catalyst

Mansour Binandeh,[✉] * Mohammad Ali Nasseri[✉] and Ali Allahresani[✉]

The aim of the project was to design and synthesize a magnetic nanocatalyst with a new organic ligand to perform the Suzuki reaction. To perform the carbon–carbon coupling reaction, the heterogeneous surface of the magnetic nanoparticles, which was in the blue phase, transferred the reactive materials to the blue phase. In the structure of this magnetic nanocatalyst, two metals, nickel and cobalt, are coated on the surface of the catalyst by the organic ligand, creating enough space to carry out the reaction, accelerate it and produce products with high efficiency. Due to the complete review of the results, the percentage of products is greater than 97% and the catalyst can be recovered during ten reuse cycles and shows a high efficiency, retaining 96% of its power. The high efficiency of the magnetic nanocatalyst in performing the reaction is very impressive and it is easily separated from the reaction medium by an external field, without causing toxic effects in the reaction and without side reactions.

1. Introduction

During the last few years, the attention of researchers has been drawn to work in the field of nanotechnology to synthesize nanocatalysts with high catalytic power in accelerating various organic chemistry reactions. One important thing that has always attracted the attention of researchers is the fabrication and optimization of the size of nanoparticles, which is required to create homogeneous and heterogeneous catalyst surfaces. As previous research has shown, the size of nanoparticles on the nanoscale ranges from just under 20 nm for the medical industry to closer to 100 nm for the chemical industry. Also, the surface of the catalyst should be large so that all kinds of coatings, ligands and metals can be applied to it to complete its catalytic structure.¹

As has been determined many times from research results, nanoparticles are divided into different types, the most important of which include: MOFs, and mesoporous and magnetic nanoparticles. Among these, magnetic nanoparticles are very remarkable due to the cheapness of the materials they are made from (including iron salts), their accessibility, the placement of a large number of ligands and metals on their substrate, and their easy removal by an external field. Also, these nanoparticles, which have a core/shell structure, can be used to create magnetic nanocatalysts that have many applications in the field of medicine, such as purification of enzymes, absorption and release of pharmaceutical biomolecules, and targeted drug delivery.^{2–6}

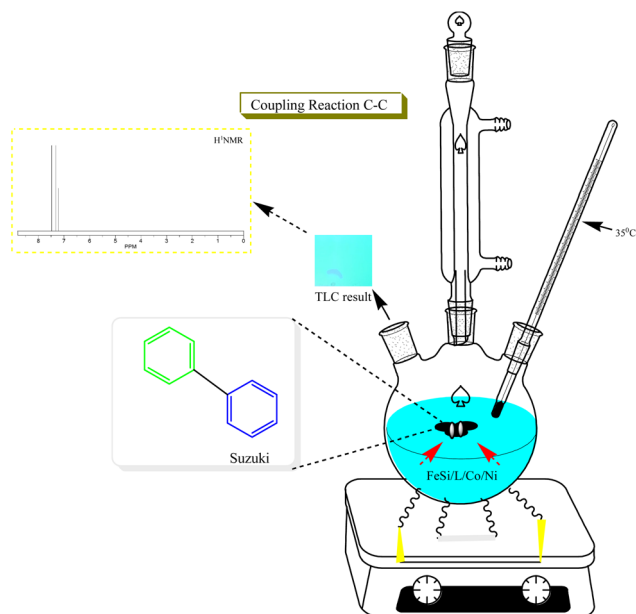
In order to increase the efficiency of magnetic nanocatalysts, their heterogeneous surface should be insulated first with a coating such as silica in order to avoid excessive oxidation of the surface by the environment and prevent it from becoming lumpy (that is, damage to the core/shell structure). Also, the presence of this silicate coating increases the efficiency of its surface in performing various chemical and biochemical reactions and also provides it with a biocompatibility property that has antibacterial effects.^{7–11}

The main difference between magnetic nanoparticles lies in the ligands that are coated on their surface, and in general, a magnetic nanocomposite consists of two core and shell structures, the core of which is magnetite nanoparticles with a silica coating (which is also the goal of this project). The core shell is formed by ligands and metals. A variety of ligands have been used until now, each of which has its own unique properties, some being made of natural materials and others of synthetic materials. The organic ligands considered in this project must have amide and amine bonds to easily connect to the surface of the catalyst and improve the performance of the nanocomposite.¹²

So far, the structure of the nanocomposite, similar to the structure of its ionized liquid, can achieve many reactions without metals, but the existence of a series of problems has resulted in an urgent need for metal nanoparticles. One of the major problems of the ionic liquid is the low percentage of products obtained, the long time spent on the reaction and the change in the pH of the ligands in different acid–base conditions. One of the most widely used metals is palladium, which performs all kinds of reactions with high speed and good efficiency, but its disadvantage is that it is expensive. Therefore,

Basic of Science, Chemistry Department, University of Birjand, Iran.
E-mail: mansurstrong@gmail.com, mansour.binandeh1987@birjand.ac.ir





Scheme 1 Suzuki coupling reaction using magnetic nanoparticle catalyst.

the use of metal nanoparticles such as copper, cobalt and nickel has been expanded.¹³

In 2010, Suzuki obtained a product from the reaction of aryl halides with phenylboronic acids, which he did for the first time. The result of this reaction was the creation of a bond between two carbons of two reactants, which became known as Suzuki's carbon-carbon coupling reaction and won him the Nobel Prize.¹⁴ The products resulting from this reaction have been widely used both in the chemical industry and in medicine, and new examples of these products have anti-fungal and anti-viral properties in the medical industry.^{15,16}

In this project, the main objective is to organize the Suzuki reaction process in such a way that under ideal conditions, with a magnetic nanocatalyst (iron@silica/organic ligand/cobalt/nickel) in an optimal amount (0.02 mol%), with the main part of the Suzuki reaction acting on reactants with electron-donating and electron-withdrawing groups, at a temperature below 40 °C, using a standard base and a green solvent, products can be obtained with a high efficiency of 97%. Also, an overview of the reaction process is provided along with ¹H-NMR analysis, which confirms the Suzuki reaction product (Scheme 1).

2. Materials and methods

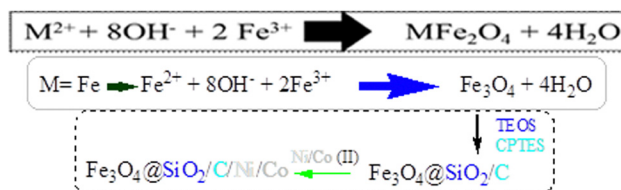
All reagents used met the necessary standards, and the solvent used was deionized water at 18 MΩ cm⁻¹. C₁₉H₁₅N₃O₂ (molecular weight 333.89 g mol⁻¹, 99.999% purity), C₄H₆NiO₄ (molecular weight 176.8 g mol⁻¹, 99% purity), C₄H₆CoO₄, (cobalt(II) acetate, molecular weight 177.02124 g mol⁻¹, 99% purity), and CPTES (molecular weight 198.72, 97% purity) were purchased from Sigma Aldrich (St. Louis, Michigan, USA). FeCl₂·4H₂O, Fe(Cl)₃·6H₂O, deionized water, argon gas, NaOH (34% aqueous

solution), TEOS, HCl, and methanol were purchased from Sinopharm Chemical Reagent Co. (Shanghai, China).

Powder XRD of the prepared catalyst was performed using a Philips PW 1830 X-ray diffractometer with a Cu Kα source (λ = 1.5418 Å) in the Bragg angle range 10–80° at 25 °C. FTIR spectra were obtained using an FTIR spectrometer (Vector 22, Bruker) in the range 400–4000 cm⁻¹ at room temperature. SEM analysis was conducted using a VEGA/TESCAN KYKY-EM 3200 microscope (acceleration voltage of 26 kV). TEM experiments were conducted using a Philips EM 208 electron microscope. EDX analysis of the catalyst was conducted using a VEGA3 XUM/TESCAN. TGA was performed using a Stanton Red Craft STA-780 (London, UK). NMR spectra were obtained using a Bruker DRX-400 instrument (300.1 MHz for ¹H-NMR, 75.4 MHz for ¹³C-NMR). The spectra were obtained using CHCl₃-d₁ as a solvent. Magnetic measurements were carried out using a VSM instrument (MDK, model 7400). Melting points were evaluated using an Electrothermal 9100 apparatus.

2.1. Nanoparticle synthesis method

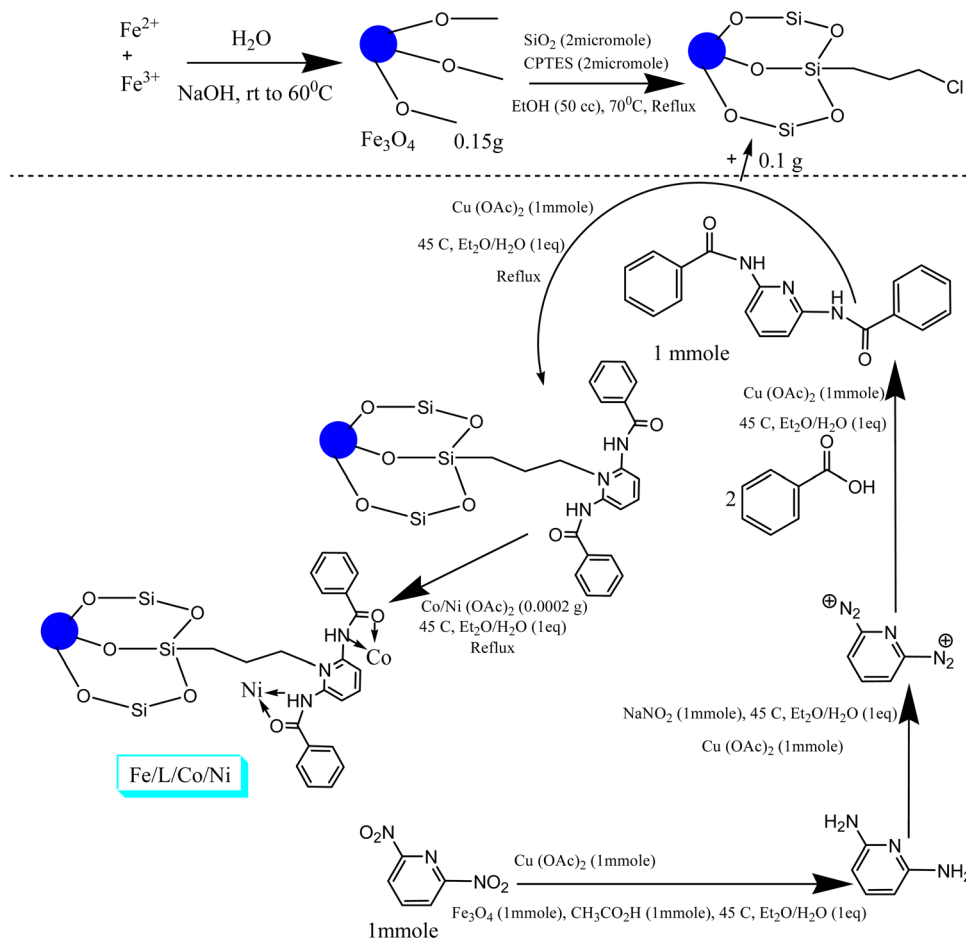
One cost-effective method for the synthesis of magnetic nanoparticles is the chemical co-precipitation method,^{7–11} which is a simple and standard method based on the heterogeneous synthesis of the nanocomposite. For its synthesis, iron(II) and (III) salts are mixed with each other at a ratio of 1 : 2 to obtain a mixture for the structure of the catalyst core (magnetite) in the aqueous phase at room temperature (25 °C), based on the following equation.



2.2. Synthesis of Fe₃O₄ magnetic nanoparticles

The first step in the synthesis of magnetic nanoparticles, amounts of 0.9 mol% FeCl₂·4H₂O salt and 1.8 mol% FeCl₃·6H₂O salt were added to 350 cc of distilled water under normal temperature conditions (25 °C) for a fixed period of 2.5 hours. After this period of time, the temperature was raised to 57 °C and the moment the temperature reached 57 °C, 4.5 cc of 10% sodium hydroxide was added to the reaction solution and the reaction continued for another 2.5 hours. Finally, the product was separated from the reaction solution with a magnet and washed with 2 cc of distilled water and 1 cc of Merck ethanol, respectively, until the excess hydroxyl groups were separated from the surface of the catalyst and the pH reached close to that of water. Then it was placed in an oven at a temperature of 60 °C for 12 hours to lose surface water, then it was placed in a vacuum oven at a temperature of 57 °C for one and a half days to lose its internal water. Finally, the completely dried (yellowish brown) product was separated from the reaction mixture





Scheme 2 Synthesis of Fe@L/Co/Ni magnetic nanoparticles.

and collected. These were the magnetic nanoparticles of magnetite.

2.3. Nanoparticle core/shell structure with metal coating

First, 0.15 g of magnetite magnetic nanoparticles were weighed, dissolved in a separate container with 25 cc of distilled water and stirred in a sonicator at room temperature (25 °C) at normal intensity for 2 hours. Then 2 cc of ethanol along with 1.5 cc of TEOS nanoparticles were added to the reaction mixture and dissolved for 1.5 hours. In the next step, 0.5 cc of 5% sodium hydroxide was added to the reaction mixture and the reaction continued for another 1.5 hours. Finally, the reaction mixture was treated as in the previous step and was made into a powder. Next, trimethoxysilyl propyl chloride ligands and $C_{19}H_{15}N_3O_2$ ligands, 1 mL of each, were added, first the first ligand, then the second ligand, and dissolved in 50 cc of ethanol. Then, in another container, 0.075 g of silica-coated magnetite nanoparticles were dissolved in 25 cc of distilled water, and added to the mixture containing the ligand and refluxed at 70 °C for one day. The next day, the obtained catalyst was washed and dried, and 0.7 g of it was dissolved in 35 cc of distilled water, with 1 mmol of $C_{19}H_{15}N_3O_2$ ligand in 10 cc of diethyl ether and 1 mmol of copper(II) acetate catalyst was

refluxed at 45 °C for one day and night. In the next step, the prepared nanocatalyst was completely washed and the catalyst dried again. This time 0.06 g of catalyst was twice dissolved in 30 cc of distilled water, first dissolving 0.0002 g of cobalt(II) acetate in 10 cc of the solvent ethyl ether, refluxing at 45 °C for 12 hours, then adding 0.0002 g of nickel to the reaction vessel and refluxing for another half day. Finally, the final product was washed several times with 5 cc of distilled water and 3 cc of Merck ethanol and dried and collected as in the previous steps. Its magnetic strength was tested with a magnet. Of course, this test analyzed all stages of the synthesis of magnetic nanocomposite, and the tests showed that its magnetic strength gradually increases because the structure of the nanocomposite becomes more complete and regular (Scheme 2).

3. Results and discussion

3.1 Detection of the structure of the magnetic nanoparticles

The magnetic nanocomposites with dimensions close to 100 nm, after synthesis, were analyzed by a series of tests to confirm their structure. The structure of the magnetic nanoparticles composed of a core/shell was investigated by FESEM,



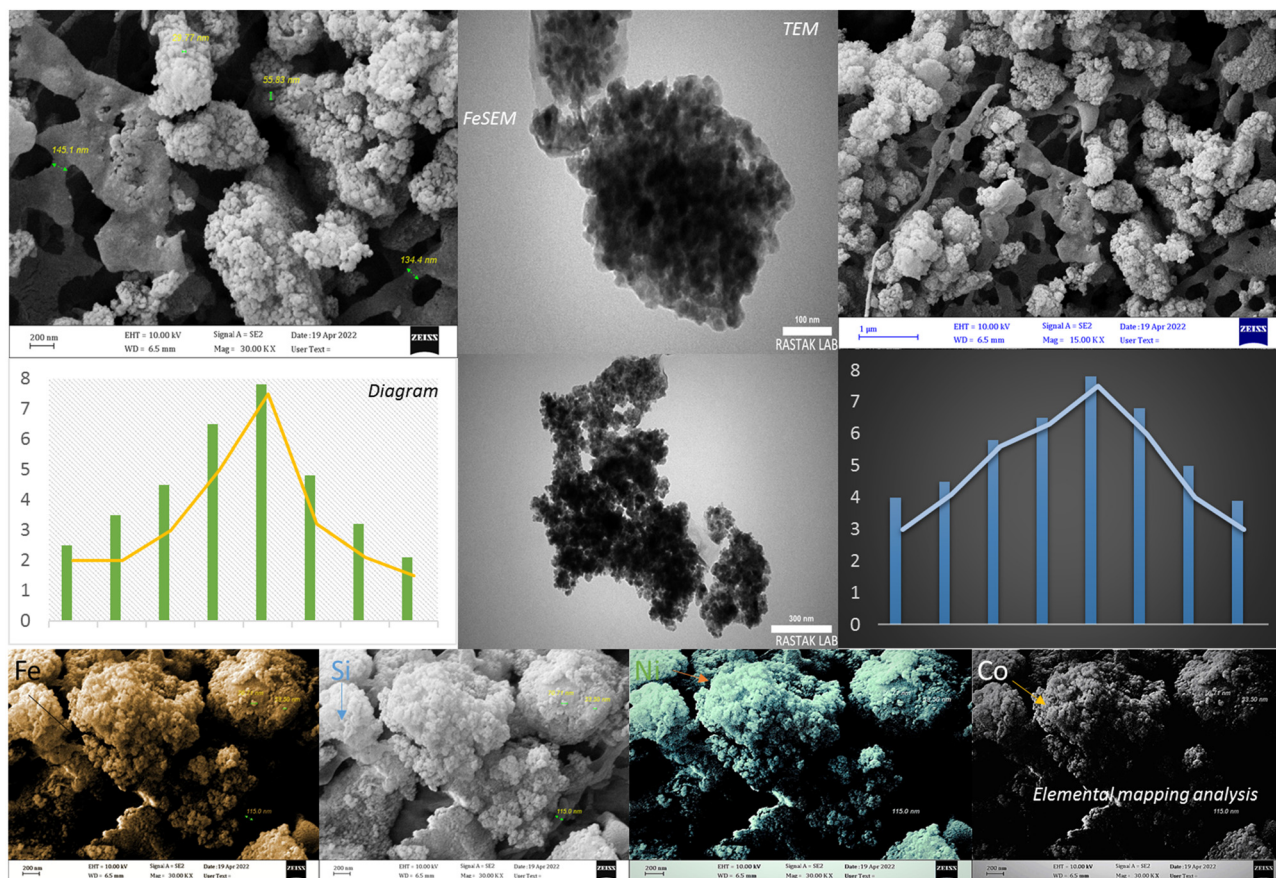


Fig. 1 TEM, FESEM and elemental mapping analyses with a graph representing the order of nanoparticles.

TEM, VSM, EDX, XRD, FTIR analyses, and the results are fully presented below.

3.2. Analysis tools of detection

3.2.1. FESEM, TEM and elemental mapping analyses.

FESEM analysis produces images of the inner surface of the nanocomposite that show the morphology and placement of all kinds of particles, so that in elemental mapping analysis, the presence of iron, silicon, cobalt and nickel metal particles is depicted, how they are dispersed and how they are connected. They show the surface of the catalyst. Also, in the TEM analysis, images of the outer surface of the nanoparticles are shown, which depict the general shape of the nanocomposite and the core/shell shape of the catalyst on a 100 nm scale. The data in the diagram also shows that the size of the nanoparticles is close to 80–90 nm, which is very favorable (here, the numbers are multiplied by ten to accurately calculate the size of the nanoparticles) (Fig. 1).

3.2.2. FTIR analysis. FTIR analysis is used to identify functional groups that have a profound effect on the structure of a compound. For this purpose, all functional groups in the magnetic nanocomposite structure were evaluated in the range of 400–4000 cm^{-1} . The results showed that the oxygen–iron band was visible in the range of 500 cm^{-1} (nanocomposite core structure), which gave a broad peak that became sharper with

placing of the silica coating, and a relatively strong peak in the range of 1000 cm^{-1} appeared for the silicon–oxygen–silica bond. Also after adding the triethoxypropylsilyl chloride ligand, a bifurcated peak appeared in the range of 1100 cm^{-1} , which is related to the carbon–chlorine bond. With the addition of the $\text{C}_{19}\text{H}_{15}\text{N}_3\text{O}_2$ ligand, an attack was made from the pyridinium nitrogen to remove the halogen chloride, so that the nitrogen–carbon band had a medium peak in the range of 1414 cm^{-1} (which was slightly shifted towards the weak field due to the resonance between the two carbonyl and amino groups). Also, in the ranges of 2900, 3100 and 3400 cm^{-1} , for carbon–hydrogen bonds, sp^3 was related to propyl, sp^2 was related to phenyl rings, and the oxygen–hydrogen band was related to hydrogen bonds, and the coating of Co/No had peaks in 574–638 cm^{-1} . According to the IR diagram data, the sharp and medium peaks confirm the general structure of the magnetic nanocomposite, which is obtained without any error and so its regular structure is confirmed (Fig. 2).

3.2.3. EDX analysis. To calculate the molar percentage of the elements, EDX analysis is used to calculate the loading and presence of elements in the nanocomposite by multiplying the molar percentage of the elements by the mass number, which is based on the keV unit. Also, by using this analysis, the relationship between the elements and the type of bond between them can also be evaluated, so that wherever two peaks of several



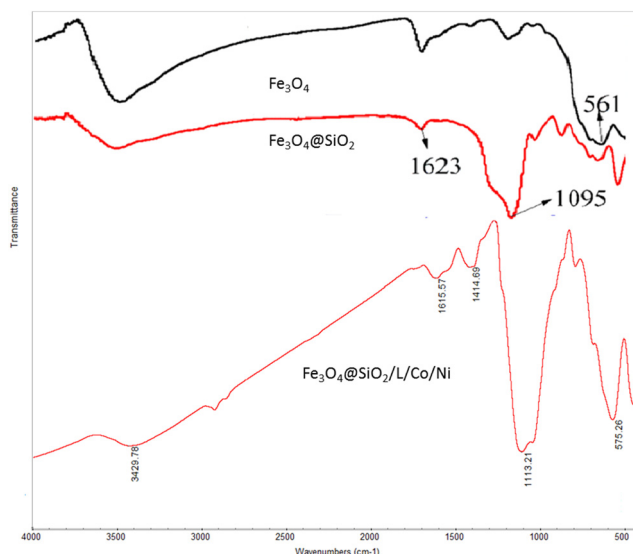


Fig. 2 FTIR analysis: (a) Fe_3O_4 ; (b) $\text{Fe}_3\text{O}_4@\text{L}$.

elements are placed on top of each other, it can be assumed without any doubt that they are related to each other, like the bond between silicon and oxygen (Fig. 3).

3.2.4. The XRD spectrum of $\text{Fe}_3\text{O}_4@\text{L}/\text{Co}/\text{Ni}$. XRD analysis widely expresses the electron transitions from the inner layers to higher levels with 2 theta criteria, and grading was obtained for each detail of the nanocatalyst. For its core structure (Fe_3O_4), peaks of 30.1° , 35.4° , 43.2° , 53.7° , 56.9° and 62.9° , and also higher bands *i.e.* 220, 311, 422, 511, and 440 cm^{-1} were related to the structure of the base (Fig. 3a). When nickel and cobalt were coated on the surface of the magnetic nanocatalyst, two new peaks were observed at $2\theta = 45^\circ$ and 58° ,

corresponding to bands at 111 and 200 cm^{-1} for cobalt nanoparticles (Fig. 3b), and a peak was observed at 75.35° corresponding to the 220.006 cm^{-1} band for nickel metal coating (Fig. 3c) on the surface of the $\text{FeSi}@\text{L}$ magnetic nanocomposite. According to the shape of the XRD analysis, the results showed that after the placement of two cobalt/nickel metals on the surface of the magnetic nanocomposite, the structure of the nanocomposite became more regular and the regular and sharp peaks were related to the size of the cobalt/nickel nanoparticles in the base state (0), which is 8 nm (Fig. 3).

3.2.5. VSM analysis. VSM is a method to measure the saturation of a magnetometer according to the type of magnetic nanoparticle (para, di or ferromagnetic) which can be evaluated according to magnetic strength. VSM analysis in terms of emu g^{-1} in magnetic field units (kOe) showed the magnetism of the nanocatalyst at two temperatures of 25 and 100 $^\circ\text{C}$ in the pH range 8–12. At room temperature (25 $^\circ\text{C}$), the intensity of the peaks is higher, which means that its magnetization has decreased normally (about 45%), but at 100 $^\circ\text{C}$, the amount of magnetization has decreased by about 30%, which increases the magnetic strength and the crystalline structure of the nanocomposite. In VSM analysis, magnetic nanoparticles (Fe_3O_4) showed results of 78 emu g^{-1} at 25 $^\circ\text{C}$ and 56 emu g^{-1} at 100 $^\circ\text{C}$; also after organic ligand coating at 25 $^\circ\text{C}$, the magnetization of the nanocomposite was 57 emu g^{-1} , and at 100 $^\circ\text{C}$ it was about 35 emu g^{-1} . Finally, after placing cobalt/nickel metals on the catalyst bed at 25 $^\circ\text{C}$, the magnetic saturation was about 42 emu g^{-1} , and at 100 $^\circ\text{C}$, it was about 27 emu g^{-1} . The general results show that at room temperature, the decrease in magnetization of the nanocomposite is about 45% and at room temperature it is about 75%, which is due to the superparamagnetization of the magnetic nanoparticles so

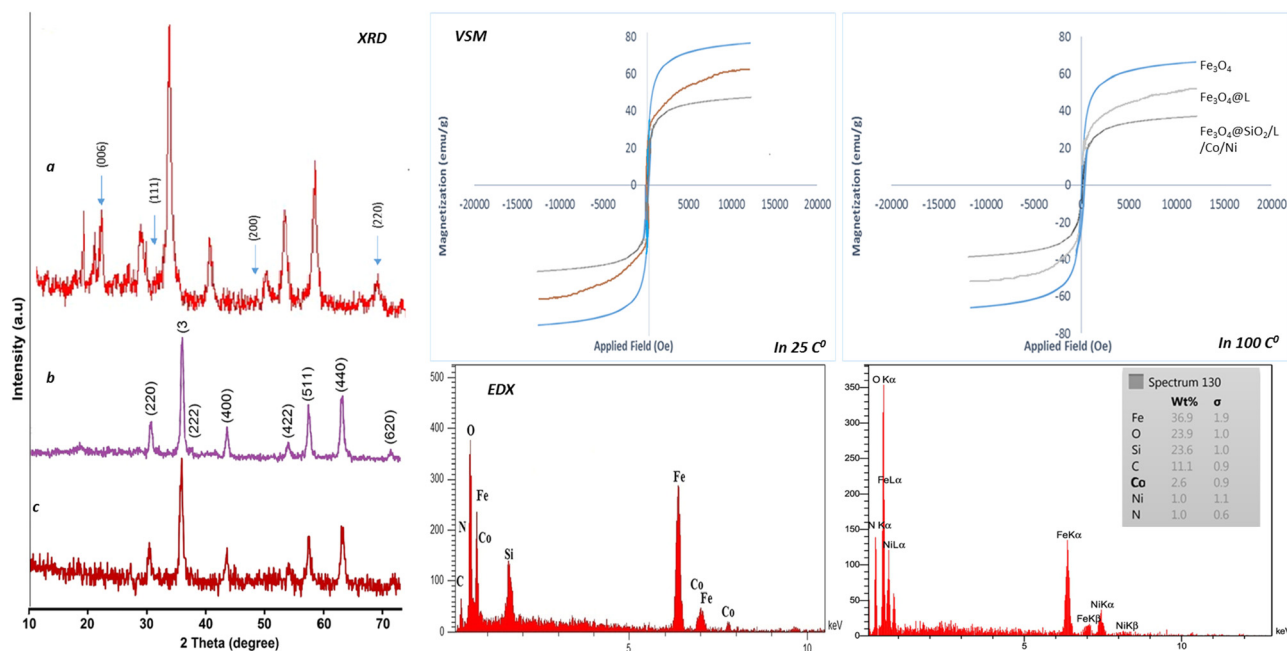


Fig. 3 EDX, VSM, and XRD spectra.



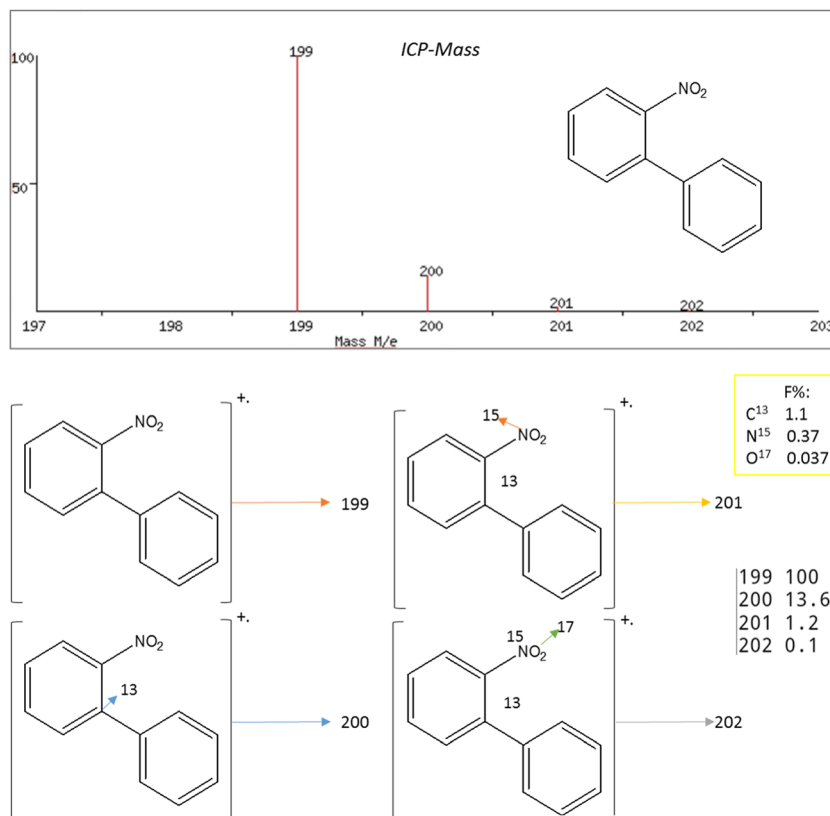


Fig. 4 ICP-mass analysis.

their efficiency increases. Also, before and after this analysis, the amount of magnetism was measured with a magnet and the results showed that even above a temperature of 100 °C, the amount of magnetism did not decrease significantly, which further confirms the magnetic power of the nanocatalyst (Fig. 3).

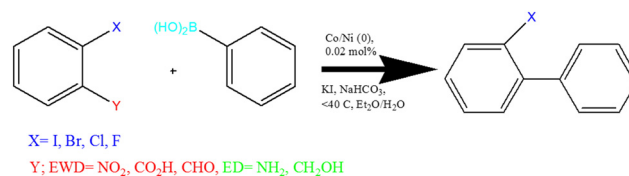
3.2.6. ICP-mass. Another very important method to evaluate the mass percentage of compounds is ICP-mass analysis, which subjects the compounds to electron bombardment to evaluate the ionic radical-carbocation with a unit of $m\ e^{-1}$ unit by mass analysis. As can be seen in Fig. 4, products and reactant containing halogen were subjected to mass spectrometry analysis to confirm the correctness of the structure of the compounds. Fluorine and hydrogen are monoisotopic, so their abundance is 100%. Carbon-13, oxygen-17 and nitrogen-15 as isotopes of the elements carbon-12, oxygen-16 and nitrogen-14 have very low abundance, so the isotopes of these elements were not visible. Therefore, the products obtained based on their structural destruction can have different mass percentages; for example, for the alpha-nitro biphenyl composition obtained, the obtained molecular ions start from the number 199 and for each carbon-13, nitrogen-15, oxygen-17. As shown in the figure, the percentage abundances of carbon-13, nitrogen-15 and oxygen-17 are very low, so the highest mass percentage is for their own mass compounds.

3.3. Suzuki reaction

In this section, after the complete identification of the magnetic nanocomposite structure, it was evaluated for the Suzuki

coupling reaction. This reaction, which is the interaction between two reagents, aryl halide and phenylboronic acid, was carried out under the conditions of basic potassium iodide salt, in diethyl ether solvent, at a temperature less than 40 °C, and was checked under standard reaction conditions (Scheme 3).

3.3.1. Optimization of the amount of nanocatalyst. One important check in a coupling reaction or any other chemical reaction is standardization of the amount of nanocatalyst. Results from studying research by other scientists have shown that the consumption of different nanocomposites depends on the type of reaction in the range of 0.2 g, which is equivalent to 2 mol%, which is not very economical for use in industry. Therefore, in this project, the synthesized magnetic nanocomposite was used in an amount of about 0.02 mol%, which is about 0.002 g, which is ideal for the reaction in industry on a scale of one ton, so only about 20 g of nanocomposite is enough. As shown in Table 1, the usage conditions of the nanocatalyst were evaluated so that at the scale of 0.5 to 2 mg



Scheme 3 Suzuki coupling reaction.



Table 1 Suzuki coupling reaction results

Entry	Salt	Solvent	Base	Cat. (mg)	Temperature (°C)	Time (min)	Yield ^a (%)	TON	TOF (h ⁻¹)
1	NaSCN	CH ₃ CN	DABCO	Fe/L/Co/Ni (10)	70	100	80	58	29
2	Cs ₂ CO ₃	THF	KF	✓10	110	120	85	68	34
3	Na ₂ CO ₃	DMSO	KF	✓5	100	75	89	62	31
4	Na ₂ SO ₂	DMF/H ₂ O (5 mmol)	NaOH	✓5	70	60	88	64	32
5	NaHCO ₃ (0.2 mol%)	Et ₂ O/H ₂ O (0.25 mmol)	KI (2mmol)	✓0.75	25	55	91	63	31.5
6	✓	✓0.5 mmol	✓	✓0.5	30	45	92	71	35.5
7	✓	✓0.75 mmol	✓	✓1	35	35	94	75	37.5
8	✓	✓1 mmol	✓	✓1.5	✓	✓	96	78	38
9	✓	✓2 mmol	✓	✓2	✓	✓	98	82	41
10	—	✓	—	Not cat.	100	120	—	45	42.5
11	NaHCO ₃	✓	✓	Fe ₃ O ₄ (20)	✓	22 h	Trace	55	27.5
12	✓	✓	✓	Fe/L (20)	✓	20	20	65	32.5
13	—	✓	—	Co/Ni (OAc) ₂ ·H ₂ O (20)	70	14	65	70	35

^a Yield refers to isolated products.

of nanocatalyst, a reaction efficiency of 91–98% is reported, which is standard. Actually, basic investigations of each detail of the catalyst before cobalt/nickel metal coating, including magnetite nanoparticles, magnetite with ligands and even a mixture of cobalt/nickel metals (alone, without binding to the catalyst) showed that at a temperature above 70 °C, the reaction took more than 12 hours and a very small percentage of product was obtained, which shows that the complete structure of the magnetic nanocatalyst in this project was about 45% superior to its catalytic constituents and about 25% higher than other nanocatalysts developed by other researchers.

3.3.2. Solvent type. Solvents play a very important role in speeding up a reaction and in mixing the reactants and the catalyst, so that in this project, in addition to water solvent (which dissolves the nanocomposite), the polar solvent diethyl ether was used, which, besides being green, creates uniformity in the environment in which it reacts. Also, after mixing the magnetic nanocomposite in water in the aqueous phase, because the reactants are generally in the organic phase, diethyl ether solvent creates a connection between the two aqueous/organic phases. Therefore, 2 mmol of diethyl ether solvent equivalent to 25 cc was used at a temperature of 35 °C, which gave the highest percentage reaction. Also, when using other solvents, which were all examined at temperatures over 70 °C,

the reaction percentage was 80%, which is very high. Diethyl ether solvent is used at a temperature below 70 °C, but by comparing this solvent with the solvents used in other research, its efficiency was about 30% higher, and it is also a green solvent (Table 1).

3.3.3. Salt. Salts are widely used to create a suitable pH in the environment, as well as to prevent the creation of unwanted compounds (due to their conductivity and also the creation of stable ions with reactive leaving groups), and among all the salts studied in this project, sodium bicarbonate was given a lot of attention due to its cheapness, good compatibility at any temperature, and availability. The results showed that using about 0.2 mol% of this salt, equivalent to 0.001 g, the reaction percentage in about 35 minutes, is greater than 97% (~98%), which was comparable with other salts used in this project. And in research by others, it has a high efficiency of about 28% and is harmless (both for the reaction itself and for the environment) (Table 1).

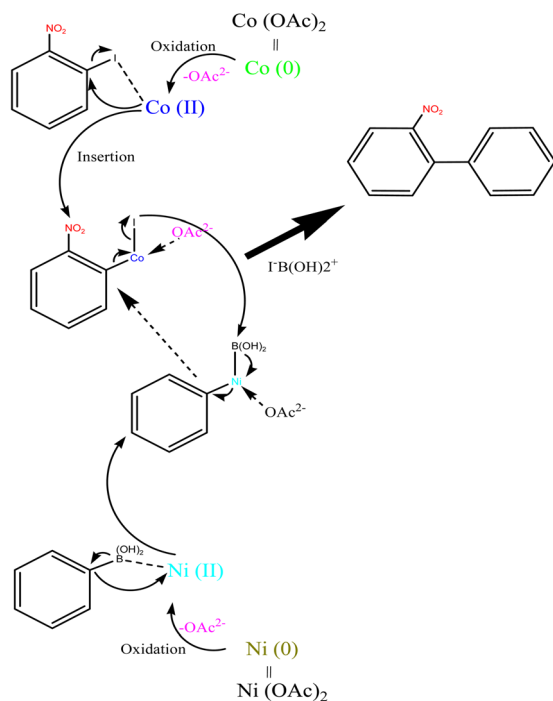
3.4. Correct identification of the obtained products

The process of the Suzuki coupling reaction has been thoroughly investigated. From the moment of starting the reaction between the two reagents, aryl halide and phenylboronic acid, it is necessary to start analysis. For this purpose, a quantity of the

Table 2 Comparison of Fe@L/Co/Ni nanocatalyst with other catalysts

Entry	Catalyst	Conditions	Time (h)	Yield ^a (%)	Ref.
1	Pd/CeO ₂ (0.01 mmol), K ₂ CO ₃ (3 equiv.)	DMF (1 mL), 90 °C	48	90	17
2	Pd (5–20 mol%), CS (10–40 mol%)	Toluene (2 mL), r.t.	24	92	18
3	Pd@COFs (100 mg)	Methanol (4 mL), r.t.	3	90	19
4	Pd (1.5 mol%), KF (0.2 mmol)	DMSO (4 mL), 100 °C	2.5	96	20
5	Pd (1.5 mol%), K ₂ CO ₃ (1 mmol)	DMSO, 80 °C	2	95	21
6	Palladium N-heterocyclic carbene (0.02 mmol), K ₂ CO ₃ (1.2 equiv.)	i-PrOH (4 mL), r.t.	6	98	22
7	Pd(OAc) ₂ /LHX (15 mol%)	DMF/H ₂ O (2 mmol), 50 °C	3	93	23
8	Chitosan/δ-FeOOH-Pd(II) (1.2 mmol)	DMF/H ₂ O (3/3 mL), 80 °C	7	95	24
9	Pd/dppf monoxide (1.0 mol) K ₃ PO ₄ ·3H ₂ O (1.5 mmol)	H ₂ O/ethanol (2 mL), 80 °C	3	98	25
10	Cross-linked poly(ITC-HPTPy)-Pd (0.23 mol%) K ₂ CO ₃ (1.5 mmol)	H ₂ O/ethanol (3 mL), 80 °C	2	98	26
11	Pd (10 mol), 3-bromo pyrazolo[1,5-a]pyrimidin-5(4 H)-one (10 mol%), DCM (1.0 mL)	Cs ₂ CO ₃ (2.0 equiv.), r.t.	24	91	27
12	Pd/Ag (0.1 mol%) K ₂ CO ₃ (3 mmol)	Ethanol (3 mL), 80 °C	1.5	92	28
13	Fe@L/Co/Ni (0.02 mol%)	Et ₂ O/KI, 35 °C	0.3–1	98	Present

^a Yield refers to isolated products, ref. 17–28.



Scheme 4 Mechanism of Suzuki coupling reaction.

reacting solution was taken at times zero, 5, 10, 15, 20, 30 minutes, 1 hour, and 2 hours, diluted for 4, 6, 12, 72 hours in a flask with ethyl acetate solvent and stained on TLC paper from the control samples of the reaction *i.e.* aryl halide, phenylboronic acid and the reaction product by a capillary tube. Then the TLC paper was transferred to a container containing the solvents ethyl acetate, *n*-hexane and methanol in a ratio of 4 : 15 : 10 drops of each and the solvents allowed to

spread over it. Finally, after the surface of the TLC paper was dry, it was placed under UV light to determine the path separating the stains from each other. The reaction is complete if all reactants have been converted into products (carbon-carbon coupling products). The examined results for all compounds along with their efficiencies are shown in Table 2. As described below, a series of reactants have electron-donating and electron-withdrawing groups on their phenyl ring and, according to the data in Table 2, it was found that the efficiency of the products with the presence of electron-withdrawing groups (cyanide, tri-nitro, di-nitro, nitro, carboxylic acid, aldehyde = electron-killing power) is far greater than that of electron donors, depending on the type of halogen group (iodine, bromine, chlorine, fluorine), in which iodine being a better leaver has turned the phenyl position into an electrophile, which is much faster for coupling taking less time with higher efficiency.

3.5. Coupling reaction process

The Suzuki reaction in this project is done by two metals cobalt and nickel, in two stages, where one of the metals (cobalt) is inserted with aryl halide and the nickel metal is inserted with phenylboronic acid. The result of the reaction is two leaving groups, ion chloride and boronic acid, which can react with each other and separate from the reaction medium.

3.6. Comparison of mechanism, recovery and reuse of nanocatalysts

In Scheme 4, the general mechanism of the Suzuki coupling reaction is described as follows: two metals coated on the magnetic nanocomposite substrate are oxidized separately from the basic state (0) during the oxidation reaction to state

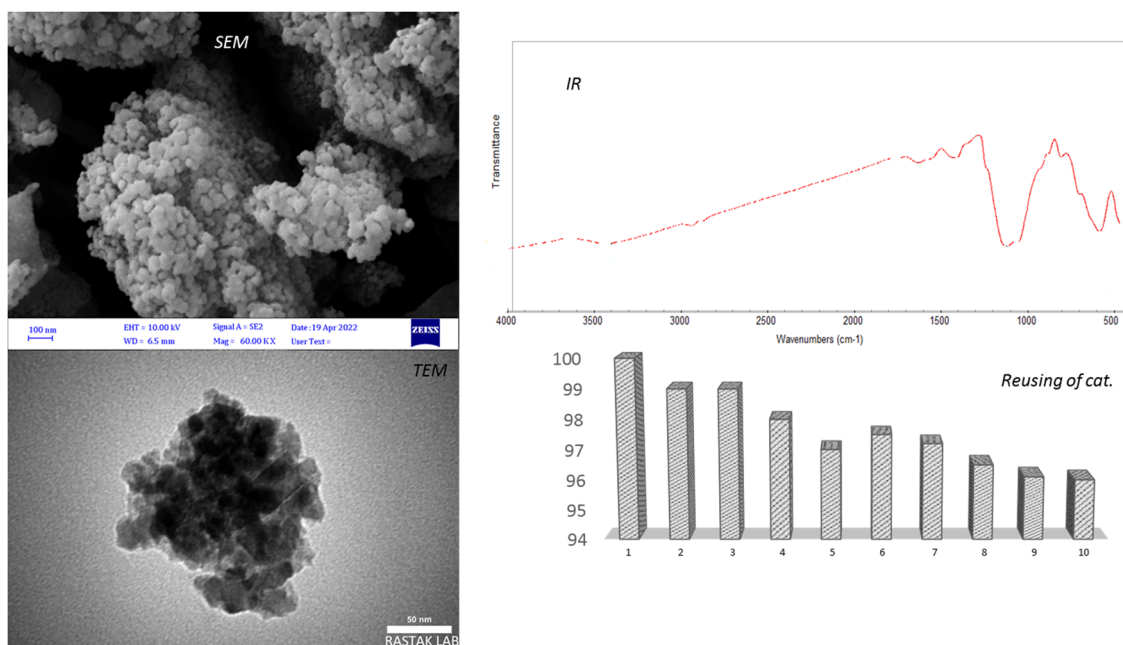
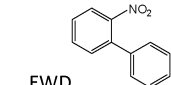
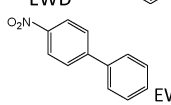
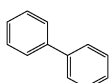
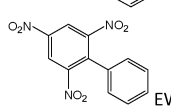
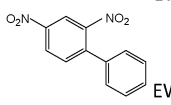
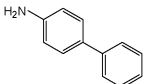
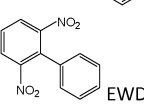
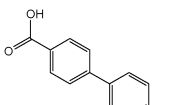
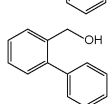
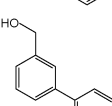
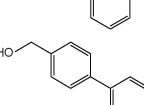


Fig. 5 IR, SEM, and TEM analyses of Fe@L/Co/Ni nanoparticles after being reused 10 times.



Table 3 Derivatives provided by the Suzuki coupling reaction

Entry	Arylhalide + phenyl boronic acid	Product	Time (min)	Yield ^a (%)	TON	TOF (h ⁻¹)	Found	Reported melting point °C
1	<i>ortho</i> -NO ₂ PhI		35	98	87	43.5	102–104	102.8
2	<i>para</i> -NO ₂ PhI		45	96	86	43	102–104	103.2
3	PhI		55	95	95	47.5	Oil	Oil
4	2,4,6-tri-NO ₂ PhI		45	98	71	35.5	345.68	345.7
5	2,4-di-NO ₂ PhF		55	97	68	34	201.9	202
6	<i>para</i> -NH ₂ PhCl		1.3 h	94	58	29	100.12	100.2
7	2,6-di-NO ₂ PhF		60	96	67	33.5	201.8	
8	<i>para</i> -CO ₂ HPhCl		70	96	61	30.5	134.77	134.8
9	2-CH ₂ OHPhI		80	95	101	50.5	88.95	89
10	3-CH ₂ OHPhBr		90	94	114	57	88.98	89.2
11	4-CH ₂ OHPhI		75	96	121	60.5	89.1	89.5

^a Yield refers to isolated products.

(II), in the next stage of the orbitals The blanks of these metals can be surrounded by the halogen group of the aryl halide compound for cobalt metal, and the acidic boronic group of the phenylboronic acid compound for nickel metal and separated from their compounds. Then the metals themselves are linked to the corresponding compounds from the same position of the leaving group; the leaving groups leave the reaction, and finally two compounds along with the metals are attacked by acetate (–2) ions during the reduction reaction. Finally, during the transition stage, metals are separated from the reaction medium and during a series of electron transfers, carbon–carbon bonds are created between two different compounds, and the compounds resulting from this process are extracted from the reaction medium in a paired manner. In fact, the products have gone into the organic environment, and the metals have been

recycled in the aqueous environment to be available again to start a new reaction. Of further importance, in addition to the catalytic power of the magnetic nanocomposite with the presence of a double metal in its structure, is that the attack between the two reactive compounds is a nucleophilic attack on the electrophilic position, so that the boronic acid group is the nucleophilic position (due to itself donating electrons to the phenyl ring) and the halide group is an electrophilic position by taking its electrons from the phenyl compound (which removes its electrons, making the compound vulnerable to electron-withdrawing agents). Another important point that should be mentioned is related to the catalytic power, so for the analysis, the catalyst is reused ten times (that is, washing it every time after performing the Suzuki reaction and retrieving it for more and more reactions), which shows that after two periods of



reuse the catalytic power of the nanocomposite has decreased by only 4%. This analysis was also done with a magnet, which showed that its magnetic power did not change and this decrease was only due to the loss of catalyst during washing. Therefore, the results of this analysis showed that the catalyst has a catalytic power of more than 96%, for further confirmation of which, SAM, TEM and IR analyses were undertaken on the recycled sample, which showed that its catalytic structure had not changed at all and it was very resistant and stable against repeated use (Fig. 5). Also, a comparison of this catalyst with other catalysts in research by others in Table 3 shows that this catalyst promoted the reaction under very ideal conditions and in terms of sample amount, reaction temperature, type of solvent, time taken to complete the reaction and product efficiency of the products the catalyst were acceptable.

4. Conclusions

The main goal of this project was the design and synthesis of a bimetallic magnetic nanocomposite with a unique ligand, for which the results of IR, SEM, TEM, VSM, EDX, XRD analyses confirmed its structure. Then, the catalyst in the Suzuki reaction is the result of carbon-carbon coupling of two compounds of aryl halide and phenylboronic acid under standard conditions, *i.e.* 0.02 mol% of magnetic nanocomposite, the green solvent diethyl ether (2 mmol), a sodium bicarbonate base (2 mmol), at a temperature of 35 °C, and the results showed that the efficiency of the obtained products is nearly 98%. The compounds resulting from the Suzuki reaction are of special importance both in the chemical industry and in medicine, so that this reaction has been used a lot for the synthesis of new pharmaceutical structures, so the magnetic catalyst that was introduced in this project, due to its wide functional surface and easy separation by an external field as a first-class catalyst could be superior to other catalysts.

Availability of data and materials

The raw/processed data that supports the findings of this study are available from the corresponding author upon reasonable request.

Conflicts of interest

The authors declare no conflicts of interest.

Acknowledgements

This project was carried out in the Birjand University Chemistry Lab, Iran.

References

- 1 M. Binandeh, Full Catalysis of Fe-NPSS with Absorption, Release and Antimicrobial Properties of BMPD Biodrug In vitro, *Annals Med. Health Sci. Res.*, 2021, **11**, 1–7.
- 2 J. Yang, S. Liu, J. F. Zheng and J. Zhou, Room-Temperature Suzuki–Miyaura Coupling of Heteroaryl Chlorides and Tosylates, *Eur. J. Org. Chem.*, 2012, 6248.
- 3 D. Cartagenova, M. Ranocchiari and S. Bachmann, Highly selective Suzuki reaction catalysed by a molecular Pd–P-MOF catalyst under mild conditions: role of ligands and palladium speciation, *Catal. Sci. Technol.*, 2022, **12**, 954–961.
- 4 X. H. Li, M. Baar, S. Blechert and M. Antonietti, Facilitating room-temperature Suzuki coupling reaction with light: Mott-Schottky photocatalyst for C–C-coupling, *Sci. Rep.*, 2013, **3**, 1743.
- 5 M. Binandeh, High-Potential of the Super-Paramagnetic of Fe₃O₄ with Coating by Silica-Thiol and Immobilization by Palladium on Oxidation of Benzyl Alcohols in Aerobic System, *J. Drug Alcohol Res.*, 2022, **11**, 1–8.
- 6 M. Samarasimharseddy, G. Prabhu, T. M. Vishwanatha and V. V. Sureshbabu, Synthesis and characterization of a Pd (0) Schiff base complex anchored on magnetic nanoporous MCM-41 as a novel and recyclable catalyst for the Suzuki and Heck reactions under green conditions, *Synthesis*, 2013, 1201.
- 7 M. Binandeh, Performance of unique magnetic nanoparticles in biomedicine, *Eur. J. Med. Chem. Rep.*, 2022, **6**, 100072–100096.
- 8 M. Binandeh, F. Karimi and S. Rostamnia, Superior performance of magnetic nanoparticles for entrapment and fixation of bovine serum albumin in-vitro, *J. Health Sci.*, 2020, **30**, 599–606.
- 9 M. Binandeh, F. Karimi and S. Rostamnia, Application of magnetic nanoparticles by comparing the absorbance and stabilization of biomolecules DNA-C, L by the electrophoretic detection, *Int. J. Health Sci.*, 2021, **15**, 3–8.
- 10 M. Binandeh, F. Karimi and S. Rostamnia, Use the best of MNPS-IHSP nanoparticles with coating of ampicillin antibiotic, as bactericidal properties, *J. Microb. Biochem. Technol.*, 2019, **11**, 416–423.
- 11 M. Binandeh, F. Karimi and S. Rostamnia, MNPS-IHSPN nanoparticles in multi-application with absorption of bio drugs in vitro, *Biochem. Biophys. Rep.*, 2021, **28**, 101159–101167.
- 12 S. Sheikh, M. A. Nasser, M. Chahkandi, O. Reiser and A. Allahresani, Dendritic structured palladium complexes: magnetically retrievable, highly efficient heterogeneous nanocatalyst for Suzuki and Heck cross-coupling reactions, *RSC Adv.*, 2022, **12**, 8833–8840.
- 13 M. Binandeh, M. A. Nasser and A. Allahresani, High-Power and High-Performance Catalyst for Suzuki Coupling Reaction, *Catalysts*, 2022, **12**, 976–989.
- 14 N. Miyaura and A. Suzuki, Palladium-catalyzed cross-coupling reactions of organoboron compounds, *Chem. Rev.*, 1995, **95**, 2457.
- 15 Y.-Q. Fang, R. Karisch and M. Lautens, Efficient syntheses of KDR kinase inhibitors using a Pd-catalyzed tandem C–N/



- Suzuki coupling as the key step, *J. Org. Chem.*, 2007, **72**, 1341.
- 16 G. Bringmann, S. Rüdenauer, T. Bruhn, L. Benson and R. Brun, Total synthesis of the antimalarial naphthylisoquinoline alkaloid 5-epi-4'-O-demethylancistrobertsonine C by asymmetric Suzuki cross-coupling, *Tetrahedron*, 2008, **64**, 5563.
 - 17 B. Liu, Activating Pd nanoparticles via the Mott-Schottky effect in Ni doped CeO₂ nanotubes for enhanced catalytic Suzuki reaction, *Mol. Catal.*, 2022, **528**, 112452–112468.
 - 18 G. Wang, Metal-organic framework grown in situ on chitosan microspheres as robust host of palladium for heterogeneous catalysis: Suzuki reaction and the p-nitrophenol reduction, *Int. J. Biol. Macromol.*, 2022, **206**, 232–241.
 - 19 Y. Li, Hollow nanosphere construction of covalent organic frameworks for catalysis: (Pd/C)@TpPa COFs in Suzuki coupling reaction, *J. Colloid Interface Sci.*, 2021, **591**, 273–280.
 - 20 S. Park, Zero Energy Heating of Solvent with Network-Structured Solar-Thermal Material: Eco-Friendly Palladium Catalysis of the Suzuki Reaction, *ACS Appl. Mater. Interfaces*, 2022, **14**(36), 40967–40974.
 - 21 S. R. Aabaka, Nanocellulose Supported PdNPs as in situ Formed Nano Catalyst for the Suzuki Coupling Reaction in Aqueous Media: A Green Approach and Waste to Wealth, *J. Organomet. Chem.*, 2021, **937**, 121719–121728.
 - 22 V. M. Kassel, Heteroaryl–Heteroaryl, Suzuki–Miyaura, Anhydrous Cross-Coupling Reactions Enabled by Trimethyl Borate, *J. Am. Chem. Soc.*, 2021, **143**(34), 13845–13853.
 - 23 M. Çalışkan, Decorated palladium nanoparticles on chitosan/δ-FeOOH microspheres: A highly active and recyclable catalyst for Suzuki coupling reaction and cyanation of aryl halides, *Inter. J. Biolog. Macromolecules*, 2021, **174**, 120–133.
 - 24 P. A. Payard, Role of dppf Monoxide in the Transmetalation Step of the Suzuki–Miyaura Coupling Reaction, *Organometallics*, 2021, **40**, 1120–1128.
 - 25 L. Zhang, Liquid/Liquid Interfacial Suzuki Polymerization Prepared Novel Triphenylamine-Based Conjugated Polymer Films with Excellent Electrochromic Properties, *ACS Appl. Mater. Interfaces*, 2021, **13**, 20810–20820.
 - 26 B. Jismy, Efficient microwave-assisted Suzuki–Miyaura cross-coupling reaction of 3-bromo pyrazolo [1, 5-a] pyrimidin-5 (4 H)-one: Towards a new access to 3, 5-diarylated 7, *RSC Adv.*, 2021, **27**, 1287–1302.
 - 27 X. Li, A novel electromagnetic mill promoted mechanochemical solid-state Suzuki–Miyaura cross-coupling reaction using ultra-low catalyst loading, *Green Chem.*, 2022, **24**, 6026–6035.
 - 28 P. Bhattacharjee, Bimetallic Pd–Ag nanoclusters decorated micro-cellulose bio-template towards efficient catalytic Suzuki–Miyaura coupling reaction of nitrogen-rich heterocycles, *Green Chem.*, 2022, **24**, 7208–7219.

